JOURNAL OF MATERIALS SCIENCE 20 (1985) 2388–2398

Factors affecting the measurement of hardness and hardness anisotropy

P. M. SARGENT
Materials Group, Department of Engineering, Cambridge University, Trumpington Street, Cambridge, UK

T. F. PAGE
Ceramics and Tribology Group, Department of Metallurgy and Materials Science, Cambridge University, Pembroke Street, Cambridge, UK

By considering the observed hardness anisotropies of two different materials ((0 0 1) single-crystal MgO and an aligned Al–$CuAl_2$ eutectic), this paper discusses some of the factors controlling the shapes and sizes of microhardness indentations. Both Vickers and Knoop profile indenters have been used. In the Vickers case, the responses of differing materials along symmetrically equivalent indenter diagonals have been observed while, in the Knoop case, indentations were often observed to have width : length ratios different from that of the indenter. The observed behaviour has been interpreted in terms of differential elastic recovery on withdrawal of the indenter, and of changes in surface topography resulting from the accommodation of material displaced from the indentation (e.g. pile-up). It is demonstrated that both effects can seriously affect the sizes and shapes of hardness impressions. Further, these "extrinsic" effects are superimposed upon the "intrinsic" mechanical response and anisotropy of the test material itself. Thus, measured hardness anisotropies are a superposition of a number of effects, each important in its own right and each with its own anisotropy. Approaches have been devised which attempt to separate these extrinsic and intrinsic components of the observed hardness response. The results allow some important conclusions to be drawn concerning the interpretation of hardness values and hardness anisotropies.

1. Introduction

Microhardness tests are usually regarded as a convenient means of investigating the mechanical properties of a material in a localized and non-destructive manner [e.g. 1, 2]. Thus, despite uncertainties as to the exact stress patterns induced in different classes of material by various shapes of indenter [e.g. 2–7], microhardness tests are widely used to explore yielding and creep behaviour [e.g. 8–12], near-surface effects [e.g. 9, 13–16], indentation plasticity [e.g. 3, 17–19] and indentation fracture behaviour [e.g. 20–22].

Diamond pyramid hardness is nearly always measured from the observed size of the impression *remaining* after a loaded indenter has both penetrated and been removed from the surface. Thus the observed hardness behaviour is the summation of a number of effects involved in the material's response to the indentation pressure during loading, in the relaxation during unloading, and in the final measurement of the residual impression. Since uniform effects are expected in isotropic materials, our approach has been to examine the indentation response of two markedly anisotropic materials – an aligned Cu–$CuAl_2$ eutectic and (0 0 1) single-crystal MgO. From the observed behaviour, this paper addresses the problem of attempting to deconvolute at least some of these varied effects; that is, we have explored the extent to which it is possible to separate the intrinsic anisotropy of the material from the further anisotropic effects of

0022–2461/85 $03.00 + .12

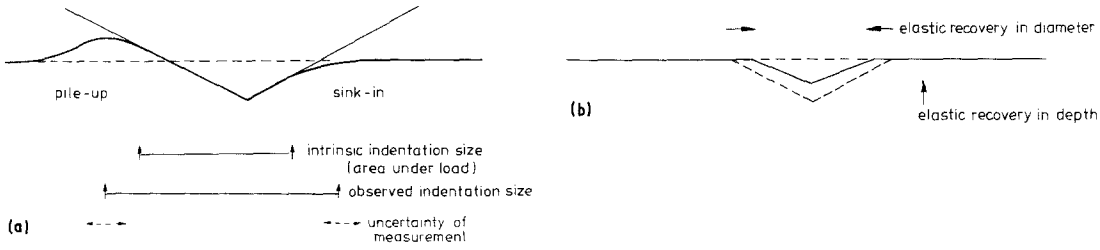

Figure 1 Extrinsic effects on indentation size and measurement: (a) Topographic effects due to "pile-up" and "sink-in" showing that the contact area, which supports the load, is not the same as the measured area, which is determined by a change in curvature of the surface and depends on the effective numerical aperature of the measuring system [2, 31, 36]. There are also likely to be observer errors in the measurement of the diagonal, independent of the numerical aperature effect. (b) Possible recovery effects are shown in the absence of other topographic changes. The impression changes in shape and size when the load on the indenter is removed due to elastic (and even plastic) recovery [2]. In most indentation tests all these effects are likely to occur.

both the pile-up of displaced material and elastic recovery.

The overall implications of extrinsic effects being superimposed on, and masking, intrinsic hardness anisotropies are important since the crystallographic variation of hardness is often used as a means of identifying slip systems in solids [e.g. 4, 23, 24].

2. Intrinsic and extrinsic factors affecting hardness

In perfectly *isotropic* materials, a number of effects are expected to control both the "load-on" and "load-off" dimensions and shapes of hardness indentations (e.g. yield stress, work-hardening, elastic recovery and creep). In such cases, it is only the shape of the indenter which determines the different responses around the identation (e.g. differing strains resulting in different amounts of elastic recovery along the long and short diagonals of Knoop indentations), but this generates no change in indentation shape as the indenter is rotated and thus no hardness anisotropy. However, in *anisotropic* materials, these controlling factors may well display individual anisotropies, including the operation of crystallographically discrete slip systems, which combine to produce an observed overall anisotropy of response to the hardness test. Thus, in order to make useful deductions concerning hardness response, some decisions must be made as to which effects are the true objects of study and which only serve to confuse the measurements required. For example, the differential surface pile-up of material displaced from the indentation can confuse the estimation of true slip anisotropies in metals and ionic solids (e.g. [25, 26] and Section 3.3), while both pile-up and differential elastic recovery can confuse the estimation of yield-stress anisotropies ([11] and Sections 3.2 and 3.3). These effects are of interest individually, so a means of deconvoluting measured data to allow their separation is highly desirable.

At this stage it is useful to define "intrinsic" and "extrinsic" effects. "Intrinsic" effects are the various responses of the material itself to the indentation being made, while extrinsic effects are those that subsequently change the size and shape of the impression finally measured. Intrinsic parameters thus include deformation character and geometry, while the principle extrinsic effects are those of elastic recovery, surface topography of displaced material, and errors concerned with measurement (see Fig. 1). It should be noted that, in addition to confusing measurement of the size and shape of the indentation, piled-up material also supports some of the load and, since "pile-up" or "sink-in" itself results from slip geometry, it is arguable whether or not this effect should be classed as intrinsic.

Since it is instrumentally impossible to completely separate all the effects, this paper will define "intrinsic" hardness as the pressure over the true area of contact of the indenter with the specimen surface, while the indenter is fully loaded and at rest with the specimen.* This is shown in Fig. 1a, from which it will be seen that this definition includes the portion of the projected area on any piled-up material.

*This definition is used for Vickers indentations, but in keeping with usual practice, Knoop hardness is calculated from the "projected" contact area, i.e. the true contact area seen in projection on the plane of the specimen surface.

To illustrate the importance of how hardness is defined, it is helpful to consider two extreme, ideal cases:

(a) a knife-like indenter, which must be aligned in a definite direction on the specimen surface, and

(b) a ball or conical indenter, for which all orientations of the indenter on the surface are identical.

For the former, the width, volume or projected area of the indentation can be used as an unambiguous, but centrosymmetric, measure of hardness with the indenter aligned along a particular direction on the surface. For the latter, the volume (or area) is the same for all indenter orientations, and in principle a hardness *anisotropy* could only be revealed by the different diameters of the indentation along particular directions caused by extrinsic effects (such as differential pile-up or elastic recovery). Since the projected contact area is the same for all orientations of ball or conical indenters, only faceted indenters can reveal any anisotropy of "intrinsic" hardness, at least as defined here.

These are extreme cases, and most commonly-used indenters fall between the two. As a consequence, either of the measurement methods (i.e. measurement of area or of diameter), or a combination of the two, can be used to define particular hardness and hardness anisotropies.

The question of measurement is fundamental to the type of data produced [e.g. 27, 28], but it has often been either overlooked or confused in the existing literature. Effects due to the different types of measurement will be discussed in Section 3.

3. Factors controlling hardness anisotropies

Before discussing the methods involved in attempting to separate some of the intrinsic and extrinsic effects combining to produce the observed hardness anisotropies, three effects need to be considered: intrinsic hardness anisotropies, and the possible effects of both elastic recovery and displaced material.

3.1. Anisotropy of intrinsic hardness

At the simplest level, anisotropy in the intrinsic hardness of materials is to be expected because the resolved stresses on the different deformation mechanisms will be different for different orientations of a faceted indenter. This presupposes that the plasticity mechanisms are crystallographically discrete and sensitive to resolved stress, e.g. dislocation slip, twinning, block shear, channelled diffusion of interstitials or crowdions, or even densification [23, 29].

Various workers have developed the Effective Resolved Shear Stress (ERSS) model whereby the stresses arising from the penetration of a crystal surface by the facets of an indenter are resolved on to the discrete deformation systems. With some success, this model has been used to predict the intrinsic hardness anisotropies exhibited on single-crystal sections, for any crystal with a single slip-system family, and tested using any faceted indenter [e.g., 4, 6, 7, 23, 30, 31].

The model ignores the pile-up or sink-in effects from displaced material, but does allow for the constraints on material displacement by the presence of the indenter. Further, the combined effects of several slip system families can be found by superposition of the calculated anisotropy curves [23]. ERSS calculations ignore whether or not the slip systems permit the accommodation of the "arbitrary strains" necessary to form a perfect indentation (i.e. to provide five independent shear strains† [32]. However, the model has been shown capable of predicting the measured Knoop hardness anisotropies on many metallic and non-metallic crystals [e.g. 4], and the measured Vickers hardness anisotropy (two-diagonal, area-estimate method) on rocksalt-structure crystals [7, 33], which is sometimes found to be the inverse of the Knoop anisotropy [4, 6].

The intrinsic anisotropy, considered as the ratio for maximum to minimum hardness values, might be expected to be greater for materials

†The question as to whether or not five independent shear deformation modes are neccessary to form an arbitrary indentation is unresolved in the literature. For single crystals, it may be possible to form an indentation by slip alone with less than five independent slip systems, if the indentation geometry is specially aligned to the slip crystallography. For polycrystalline materials, and for most real single-crystal situations, this will be improbable. However, at loads lower than those for the onset of indentation fracture, it seems possible to make crack-free indentations in all materials. How the constraint of five independent deformation modes is satisfied in these cases is unclear though elastic deformation, unusual deformation modes, limited grain boundary movement etc. might be conceived as playing some role.

with a limited number of slip systems‡. Further, and for any material, the effect should be more marked if a wedge-shaped, rather than a more regular pyramidal indenter is used. The anisotropy is expected to be less severe as mechanisms less dependent on orientation become important in determining the indentation response, e.g. densification or difussion creep. On the other hand, if many different types of orientation-dependent mechanism are active, then their combined effect could be either to accentuate or to "average out" the observed anisotropy.

In polycrystalline materials, intrinsic hardness anisotropy is to be expected (by analogy with single crystals) if the material is textured by having crystallographic ordering of the individual grains. Alternatively, if the grains are not equiaxed and have an overall shape orientation (e.g. rods and lamellae), then intrinsic anisotropy could result if the different grains and/or grain boundaries have different mechanical properties. Thus hardness anisotropy could be a useful method for investigating these types of texture, but experimental studies have generally been less than successful, largely due to insufficient development of the theoretical background [34].

Overall, a number of factors can lead to an anisotropy of intrinsic hardness. While it would be convenient to use hardness anisotropy experiments to investigate these various deformation responses, a satisfactory model only exists for shear mechanism in single crystals. Further, the intrinsic hardness anisotropy may be masked by other effects, as will now be explained.

3.2. Elastic recovery

Elastic recovery in both the depth and the faces of indentations has been clearly demonstrated by interferometric techniques as, e.g. by Buckle [25]. Strangely, recovery in the indentation diagonals has received less attention though it has been considered by Marsh [8], Sargent and Page [11], and Marshall, Noma and Evans [35]. In the plane of the surface, and for a given orientation θ of the indenter, the magnitude of the elastic recovery strain is expected to be given by the ratio of the lateral compressive stress Y induced by the loaded indenter and the "effective Young's modulus" E in the plane of the test surface, both quantities varying with orientation θ in the surface. When the loaded indenter is at rest, the lateral compressive stresses are probably similar to the flow stress of the material, and thus Y_θ is expected to be similar to the flow stress anisotropy. The higher the flow stress, the *more* the indentation can be expected to contract when the indenter is removed; whereas the higher the modulus, the *less* contraction strain is to be expected. Thus the indentation is expected to contract by an amount proportional to Y_θ/E_θ in each direction. Therefore, for a conical indenter the residual impression is expected to deviate from circularity because of the anisotropic recovery of the diameters at different azimuths θ in the surface.

For faceted indenters, the compressive stresses are expected to vary with the shape of the indenter. For Knoop indentations, very little compressive stress is expected in the line of the long diagonal (Fig. 2b) and therefore little elastic recovery is expected in that diagonal, whatever the orientation of the indenter on the surface. Thus, Marshall *et al.* [35] have suggested a means of estimating Young's modulus from the width contraction of Knoop indentations, the flow stress being estimated from the hardness. For Vickers indentations, the maximum compressive stress is expected to be normal to the faces (Fig. 2a) and there is always a strong component of lateral compressive stress in line with each of the diagonals. Hence some elastically-driven recovery is expected, and is indeed observed, in both widths and diagonals.

In plastically anisotropic materials which are fairly isotropic elastically (i.e. Al–$CuAl_2$ eutectic, which has a Young's modulus anisotropy of only about 10% [11]), the elastic recovery of any diagonal can be expected to be approximately proportional to the flow stress in that direction. This idea has been used to estimate (very approximately) the elastically-driven recovery of Vickers indentations in the Al–$CuAl_2$ eutectic [11].

‡Since there are very few, if any, cases where the active slip systems controlling hardness repsonse have been completely identified independently of the observed anisotropy (and here we would include deformation in the 'core' of the indentation besides any obvious slip activity as witnessed by slip steps, etch-pit rays etc.), we have been unable to explore this hypothesis. In many cases, the magnitude of observed anisotropies may well reflect the difficulties of initiating slip (or other deformation) on secondary systems. It is interesting to note that diamond is reported to show considerable hardness anisotropy [4] despite its apparently having five independent primary slip systems (cubic F: $\{1\,1\,1\}\langle 1\,1\,0\rangle$ slip).

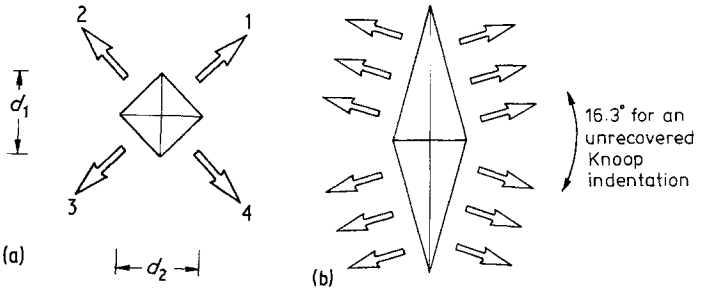

Figure 2 Plans of indentations showing the directions of postulated largest compressive stresses in the plane of the specimen surface; (a) Vickers, (b) Knoop.

Experimentally, the greatest degree of elastic recovery is always observed to be in the indentation depth [e.g. 25]; thus, Poissonian effects could indirectly cause this depth recovery to contribute further to any existing anisotropic lateral expansion or contraction of the identation.

We may conclude that while there has been a long-standing awareness of the effects of elastic recovery, the phenomenon has never really been satisfactorily modelled. Since typical recovery strains (Y/E) should be small (at most 0.03 for hard, stiff materials), they could make minor contributions to observed anisotropies and might dominate when other effects are small.

3.3. Surface topography effects

The material displaced by the indenter must flow somewhere and, for ductile materials, it usually piles up next to the indentation such that some of it also supports some portion of the load (see Fig. 1a). However, if the material has a high ratio of flow stress to elastic modulus [e.g. 7, 8, 11] or strongly work-hardens [e.g. 2, 3, 7], then the material immediately adjacent to the indenter may be displaced radially, sometimes forming a "sink-in" (see Fig. 1a). Such topographic effects can affect the measurement of indentation diagonals, as it is often difficult to determine at which point the pile-up (or sink-in) no longer supports the load. This is the case whether light microscopy or scanning electron microscopy (SEM) observations are made, and such effects provide errors additional to those due to optical limitations [e.g., 36, 37]. These topographic effects are the most likely cause of indentations apparently displaying markedly different shapes from the indenters which made them, e.g. the "barrelling" or "pin-cushioning" of Vickers indentations. Thus, in aligned Al–$CuAl_2$ the observed shape difference is almost certainly due to pile-up, as the effects are about 200 times too large to be due to simple elastic recovery [11].

In single crystals, where the crystallography of slip is important, very complex patterns of surface relief can be formed as material is moved away from differently-shaped indenters by the action of discrete slip systems. This has been dramatically illustrated by Armstrong and Wu [26] on (0 0 1) surfaces of MgO single crystals, where it was shown that around Vickers indentations, the surface grooves radiating along ⟨1 0 0⟩ directions and piled-up ridges radiating along ⟨1 1 0⟩ directions correlated with the expected slip activity. However, the multiple-beam interferograms of Boyarskaya *et al.* [31] of Knoop indentations in the same material showed no grooves at all along ⟨1 0 0⟩ directions, pile-up only being observed at the ends of the short diagonals for all indenter orientations.

The pile-ups surrounding both Knoop and Vickers indentations are known to become less distinct, smoother and more rounded as the indentations are made smaller [7]. The sharply-edged grooves and ridges observed by Armstrong and Wu [26] were not present around the 50 gf (0.49 N) Vickers indentations made in MgO in the present study, but were observed at higher loads (Fig. 3).

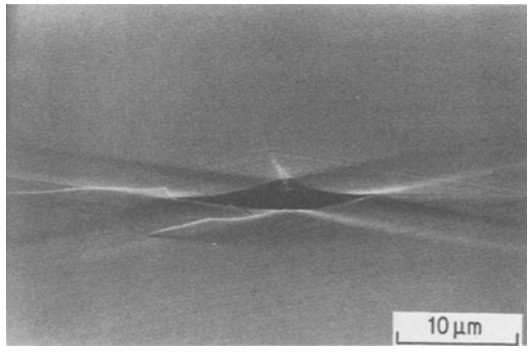

Figure 3 SEM micrograph of a Vickers indentation on the (0 0 1) surface of a MgO crystal. The indentation diagonals lie along ⟨1 1 0⟩ directions. Slip steps on those {1 1 0} planes at 45° to the surface can be seen, as can cracks on the {1 1 0} planes at 90° to the surface. The indentation was made using a 100 g load, (75° tilt and 30 kV).

Intrinsic hardness anisotropies due to crystallographic slip in single crystals have been measured to be between about 2% and 50% [4]. Pile-ups can affect the hardness by up to about 30%. The maximum elastic recovery is limited by the material's theoretical strength (about $E/30$) which would lead to an absolute maximum diagonal contraction of 3% and a hardness recovery of 6%.

Thus, both extrinsic effects are likely to be important but need careful observation to detect their presence.

4. Experimental procedure

Microhardness indentations were made with a Leitz Miniload machine using loads of 50 gf (0.49 N) and 100 gf (0.98 N), and Vickers and Knoop indenters. Six indentations were made at each orientation under room-temperature and ambient-atmosphere conditions. The indenter velocities on contact and during load application were estimated to be 100 μm sec^{-1} and 30 μm sec^{-1} respectively, with a dwell-time at full load of 10 sec. Indentations were measured at normal incidence using the light microscope on the Miniload. SEM micrographs were also taken using a Cambridge Instruments S II (eutectic samples) and Camscan 4 (MgO single crystals). The MgO was sputter-coated with gold prior to both light microscopy and SEM examination.

The Al–$CuAl_2$ directionally solidified eutectic sample was made by Dr D. C. Tidy [38] and the MgO single crystal was supplied by Dr Sambell of AERE Harwell; it was originally grown by Semi-Elements Inc. These materials are the same as those used in previous studies of Indentation behaviour [7, 11, 39].

The MgO was cleaved across a (1 0 0) plane and the eutectic was cut perpendicular to the solidification direction. Both materials were mechanically polished down to 0.1 μm with diamond paste. After polishing, the MgO was washed in water and acetone, and dried in hot air immediately prior to indentation.

Microhardness is sensitive to indentation size and chemomechanical effects (because of different proportions of the plastically-deforming volume being close to the surface); to dwell-time, and probably to indenter velocity (because of anomalous indentation creep [9, 13, 14, 39]. All these effects were considered, and all indentations were made at the same time under the same conditions for each of the two materials.

5. Calculation of hardness numbers

Conventionally, Knoop hardness is derived from a single long-diagonal measurement whereas Vickers hardness is derived by taking a mean (arithmetical or geometrical [7, 40]) of the two orthogonal diagonals. In both cases, hardness numbers are calculated by converting these diagonal measurements into areas (contact or projected), assuming ideally-shaped indentations. However, as was shown in Section 3.3, and particularly for anisotropic materials, indentations rarely have the same ideal shapes as the indenters that made them. Even in the case of Vickers indentations, it often occurs that the two diagonal lengths are not sufficient to determine the true contact area (e.g. for "pin-cushioned" or "barrelled" indentations). In order to allow for deviations from the ideal shapes, Blau [27, 28] has proposed a projected-area hardness calculated from the actual measured area of indentations.§ However, such measurements still include the effects of extrinsic factors such as pile-up and elastic recovery, together with their individual anisotropies, summed over all directions around the indentation. With this in mind, our approach has been to consider only individual directions so that we might try to separate intrinsic effects associated with that one direction. Thus the hardness numbers presented in this paper are generally calculated by a single-diagonal method, i.e. by inserting the relevant diagonal measurement d into one of the following equations:

$$\text{Vickers} \qquad H_V = 1854.4L/d^2 \qquad (1)$$

$$\text{Knoop (length)} \qquad H_{K_d} = 14230L/d^2 \qquad (2)$$

$$\text{Knoop (width)} \qquad H_{K_w} = 281.175L/w^2 \qquad (3)$$

where L is the applied load in gf, d or w the relevant diagonal in μm and H the hardness in kgf mm^{-2} (1 kgf mm^{-2} = 9.81 MPa). Equations 2 and 3 are related by a factor of $(7.114)^2$, since ideally a factor of 7.114 relates the long and short diagonals of a perfectly formed Knoop indentation.

For any "one-diagonal method" of indentation hardness-anisotropy measurement, a specific direction in the surface of the test material must be chosen as a reference direction. These were the ⟨1 0 0⟩ directions for the MgO (0 0 1), and the

§Specifically for indentations misshapen by indenter misalignment, Moore [40] suggested calculating the Vickers hardness from the *geometric* mean of the two diagonals.

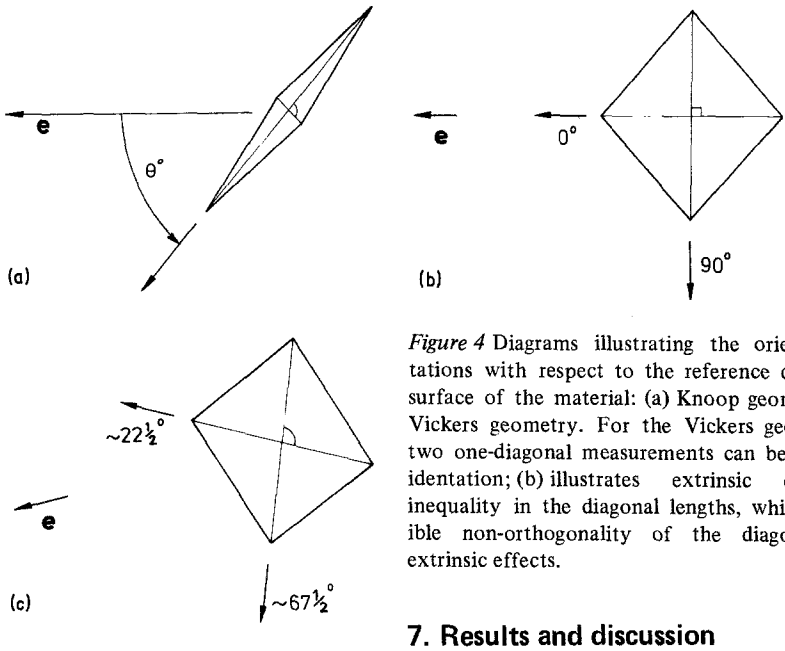

Figure 4 Diagrams illustrating the orientation of identations with respect to the reference direction e in the surface of the material: (a) Knoop geometry, (b) and (c) Vickers geometry. For the Vickers geometry note that two one-diagonal measurements can be made from each identation; (b) illustrates extrinsic effects creating inequality in the diagonal lengths, while (c) shows possible non-orthogonality of the diagonals, also from extrinsic effects.

lamellae alignment direction e in the eutectic [11]. The orientations of indentation diagonals were defined as being at an angle θ to the reference direction as defined in Fig. 4. Whilst this is unique for the Knoop indentation shown in Fig. 4a, pairs of different "one-diagonal" hardness measurements can be made from the same Vickers indentation as shown in Figs. 4b and 4c, where the diagonals are at 0°, 90° and approximately $22\frac{1}{2}°$, $67\frac{1}{2}°$ from e. Differences in the lengths of the two diagonals from the same indentation must be due to extrinsic effects.

6. Prediction of hardness numbers

In Section 7, a number of means will be employed to establish some estimate of the intrinsic hardness anisotropy for comparison with the measured behaviour. Briefly these methods are:

1. use of the ERSS model in the form developed and described by Sawyer *et al.* [23] (see Section 3.1);

2. use of bulk mechanical-property data to estimate possible hardness anisotropy from considerations of the compressive strains accommodating indentation (see Section 7.1);

3. use of the method proposed by Raghuram and Armstrong [41] to estimate a Vickers hardness value from the arithmetic mean of the hardness measured from two orthogonal Knoop indentations.

7. Results and discussion

7.1. Results for the Al–$CuAl_2$ eutectic

Fig. 5a shows the hardness anisotropies measured using the single-diagonal method for both Vickers and Knoop indenters, while Fig. 5b shows the ratio d/w of the measured long (d) and short (w) diagonal lengths for the Knoop indentations. For an ideal indentation the ratio d/w is 7.114, and deviations from this value should result from extrinsic effects. Fig. 5b shows that extrinsic effects are both pronounced and approximately constant for all orientations of the indenter, with a slight minimum at $\theta = 45°$. Since d/w is always greater than the ideal value, possible extrinsic effects causing this behaviour could be any combination of (a) more elastic contraction in the width than in the length, (b) more pile-up at the ends than at the middle, and/or (c) some sink-in at the middle of the identations. Since, in this case, the results show that the extrinsic effects are not very orientation-dependent, it seems safe to conclude that the measured hardness anisotropy reflects the anisotropy of the intrinsic hardness, though absolute hardness values will be strongly affected. Evidence for this can be seen in Fig. 5a, where the hardness values calculated form the short and long Knoop diagonals are different for any given indenter orientation; for example H_{K_d} with the long diagonal d at 90° to e gives a value of ~ 1.9 GPa, while H_{K_w} with the width w at 0° to e (i.e. the same indentation) gives ~ 1.2 GPa. Since from Fig. 5b, d/w is always greater than the ideal value, H_{K_w} is always greater than H_{K_d}, as is

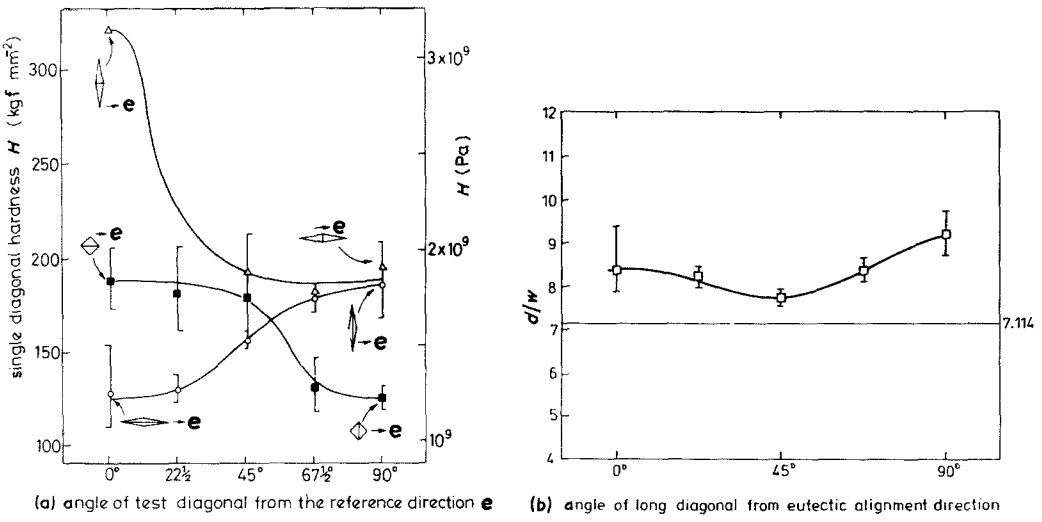

Figure 5 Results from indentations made on Al–$CuAl_2$ eutectic. Six identations were made at each orientation with a load of 50 g. (a) Hardness anisotropy of the eutectic as measured by the single-diagonal method for Vickers indentations, and for each diagonal of the Knoop indentations (■ – Vickers; ○ – Knoop (d); △ – Knoop (w)) (b) a plot showing the orientation dependence of the shape of Knoop indentations. For the Knoop data, note than when the short diagonal w is parallel to the reference direction, the long diagonal d is 90° away, i.e. the $H_{K_w}(0°)$ and the $H_{K_d}(90°)$ values are measured from the same indentation. Thus the maximum in H_{K_d} and H_{K_w} occur at the *same indenter orientation*. For changing indenter azimuths, the anisotropies in H_{K_d} and H_{K_w} are therefore similar but differ in absolute values, as witnessed by the virtually constant d/w ratio in (b).

shown in Fig. 5a where the anisotropies in H_{K_w} and H_{K_d} are similar, but different in magnitude; for example the maximum to minimum ratio for H_{K_w} is ~ 1.77, whereas that for H_{K_d} is ~ 1.44 (note the 90° "phase difference" between the curves).

For comparison, it is possible to make a qualitative prediction of the expected intrinsic hardness anisotropy from uniaxial strength data. The lowest intrinsic hardness might be expected to occur when the greatest stresses are oriented along the weakest directions in the material. By analogy with a wedge, where the greatest stresses are perpendicular to the faces, the greatest compressive stresses around a Knoop indenter would be roughly parallel to its shortest diagonal (see Fig. 2b). The lowest uniaxial compressive strength in aligned Cu–$CuAl_2$ is perpendicular to the eutectic alignment direction **e** [11, 42]; the minima of both the measured Knoop hardnesses do indeed occur at this orientation, i.e. when $\theta_w = 90°$ and $\theta_d = 0°$, and in both cases the length of the indentation is perpendicular to the direction of maximum yield stress.

Thus, for this material, substantial extrinsic effects have been found in the Knoop hardness behaviour, but in this case they do not appear to obscure the intrinsic hardness anisotropy which is consistent with the expected mechanical behaviour. Absolute values are, however, affected.

For Vickers indentations in the eutectic there seems to be no good way of estimating the intrinsic hardness anisotropy. The measured single-diagonal hardness has a marked anisotropy, and there are clear changes in the indentation shape with orientation, previously reported as being due to $\sim 0.6\,\mu m$ pile-up rather than to elastic recovery [11].

It has been demonstrated above that the measured Knoop hardness reflects the intrinsic behaviour, and thus it may be possible to obtain some estimates of the intrinsic Vickers hardness anisotropy using Raghuram and Armstrong's method [41] of averaging the hardness from orthogonal Knoop indentations. Fig. 6 shows that this procedure shows negligible anisotropy, which perhaps indicates that the intrinsic Vickers anisotropy is also likely to be very small. Thus the observed single-diagonal Vickers anisotropy is probably mostly attributable to extrinsic effects, principally pile-up [11]. This is in complete contrast to the Knoop situation, where precisely the reverse holds true; in that case, the intrinsic effects outweigh the extrinsic effects.

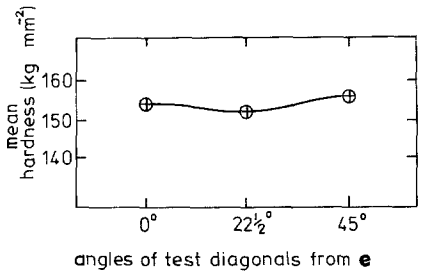

Figure 6 Estimation of the intrinsic Vickers hardness response from orthogonal Knoop indentations in Al–$CuAl_2$. Circles show the mean hardness calculated using Armstrong and Raghuram's method [6] for Knoop indentations: $H_v(\theta) = 1/2[H_{K_d}(\theta - 45°) + H_{K_d}(\theta + 45°)]$.

7.2. Results for single-crystal MgO

Fig. 7a shows the hardness anisotropies measured using the single-diagonal method for both Knoop and Vickers indenters. Fig. 7b shows the anisotropy of the d/w ratio for the Knoop indentations as before. Where d/w is less than 7.114, i.e. where the long diagonal is within 12° of the ⟨1 0 0⟩ direction, substantial cracking was observed parallel to the length of the indentation together with significant pile-up at both ends of the short diagonal. Thus the low d/w values are probably due to extrinsic effects making the short diagonal appear longer, though some slight elastically driven recovery along the long diagonal cannot be ruled out. MgO is expected to be generally more susceptible to elastic recovery than the Al–$CuAl_2$ material, since it has a Y/E ratio of approximately 0.012 as opposed to 0.0019 for the eutectic [42]. When the indentation is made with the long diagonal more than 12° away from ⟨1 0 0⟩, there is no cracking (for 50 gf = 0.49 N loads), and the surface appears absolutely flat in the SEM (as observed at high tilt). The high d/w ratios in this regime are probably due to elastic recovery in the short diagonal, as this is thought to be more likely than pile-up occurring at the ends of the long diagonal (though, in fact, only ~ 0.2 μm pile-up would be necessary to account for the observed d/w ratio of 11).

Thus, there appear to be two regimes of behaviour, depending on the orientation of the indentations. In both regimes the measured length of the short diagonal is strongly affected by extrinsic factors, but probably by different factors in each regime. Therefore the short-diagonal microhardness anisotropy cannot usefully be compared with the theoretically-derived intrinsic anisotropies. The long diagonal, however, appears to be less susceptible to pile-up and elastic recovery, and results may be compared with the anisotropies predicted for MgO (0 0 1) surfaces by the ERSS model [4, 7, 33]. Using the model of Sawyer, Sargent and Page [23], an ERSS prediction has

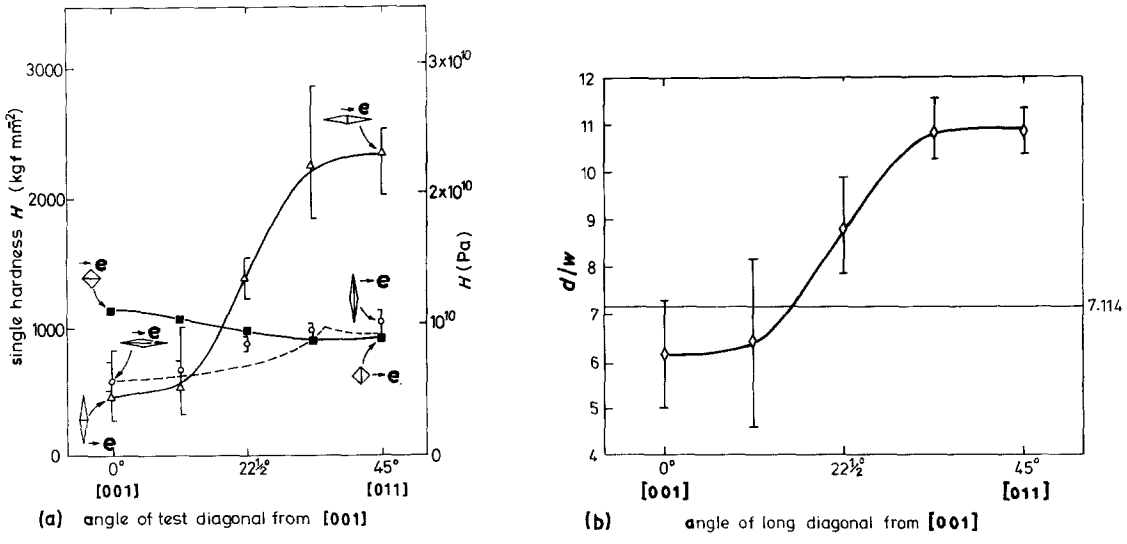

Figure 7 Results from indentations made on the (1 0 0) surface of a single crystal of MgO. Azimuths are quoted to ⟨0 0 1⟩ as reference direction, i.e. 45° is parallel to ⟨0 1 1⟩. (a) Vickers and Knoop single-diagonal hardness anisotropies and the ERSS Knoop prediction (long diagonal) showing qualitative agreement between the Knoop (d) data and the ERSS computation performed as described in [23] (■ – Vickers; ○ – Knoop (d); △ – Knoop (w); – – – ERSS Knoop prediction (scaled to agree with experiment at $\theta = 0°$); (b) a plot showing the orientation dependence of the shape of Knoop indentations.

been made for this case and is shown in Fig. 7a. It is clearly qualitatively similar to that measured using the Knoop long diagonal.

The interpretation of Vickers indentation measurements on (0 0 1) MgO surfaces is more complex than that of Knoop indentations. Firstly, the indenter has the same plane symmetry as that of the (0 0 1) section and therefore the two diagonals are always oriented along symmetrically related directions. Thus, changes in the shapes of indentations due to extrinsic effects cannot be deduced, even in principle, from simple measurements of both diagonals, as they can for Knoop indenters (or for Vickers indenters on surfaces of less than four-fold plane symmetry). Secondly, the complex slip-step surface topography around Vickers indentations (see Fig. 3 and [26]) completely masks any other extrinsic effects, such as elastic recovery, which may occur.

For Vickers indentations on (0 0 1) MgO surfaces, the two-diagonal, arithmetic-mean method of calculating hardness yields the same results as the one-diagonal method, since the diagonals are always of the same length. However, this is not equivalent to an areal measurement as the indentations have curved sides.

The measured Vickers hardness has the same anisotropy as that predicted by the ERSS models [4, 7, 33]¶; although no definite conclusions may be drawn because of the many uncertainties in the comparison, this may indicate that for this indentation plane in this material the two principle extrinsic effects, surface topography and elastic recovery, may have complementary anisotropies and may tend to compensate for each other.

As with the measurements made on the Al–$CuAl_2$ eutectic, careful analysis of the experimental data has revealed that extrinsic effects affect the hardness behaviour of MgO. However, comparisons with ERSS model predictions for both the Vickers and Knoop cases have established that intrinsic hardness anisotropies appear to dominate the experimental observations.

8. Conclusions

The results described here demonstrate the importance of making careful measurements of the final shapes of hardness indentations and the topographies of the surfaces around them. By comparison of indentation shapes with the ideal expected from the indenter, the occurrence of significant extrinsic effects (pile-up topography, elastic recovery) have been shown often to be superimposed upon expected intrinsic hardness anisotropies. We therefore suggest that careful microscopy (e.g. by Nomarski interference microscopy, SEM and stereo techniques [e.g. 44]) should ideally always accompany hardness measurements, so that material characteristics other than some "hardness number" can be identified.

This study has been made with two different materials and two different indenters, so that there are four different observed hardness anisotropies to be considered. Each of these anisotropies has been assumed to be separable into intrinsic and extrinsic factors, making eight anisotropies in all. Of these eight, the expected intrinsic Vickers and Knoop anisotropies of MgO have been calculated using the ERSS model, and the intrinsic anisotropy for the Knoop indenter on the eutectic has been estimated using a wedge analogy. Thus, only the Vickers intrinsic anisotropy on the eutectic has had to be deduced entirely from experiment. With these intrinsic anisotropies in mind, it has been found that:

1. For Al–$CuAl_2$ specimens, the observed anisotropy of Vickers hardness appears dominated by extrinsic effects, principally pile-up.
2. Also for Al–$CuAl_2$ specimens, extrinsic effects contribute to the observed anisotropy of Knoop hardness but do not dominate the intrinsic anisotropy.
3. For (0 0 1) MgO, the anisotropy of Knoop hardness seems to agree with the ERSS prediction, and extrinsic effects on the long-diagonal hardness are small. However, hardness values calculated from Knoop width measurements are dominated by extrinsic effects.
4. For (0 0 1) MgO, the anisotropy of Vickers hardness agrees well with the ERSS model. While the "barrelling" and "pin-cushioning" of indentations shows that surface topography effects exist, the total extrinsic effects seem to be either small or self-balancing.

With hindsight, there is an obvious need to carefully characterize the shape of hardness indenters prior to conducting experiments of this type, rather than simply relying on their having some standard profile.

¶ Fig. 7a shows that the anisotropies of Knoop and Vickers hardness are out of phase by 90°, as explained in Section 7.2. Though some authors have found this surprising [43], it is entirely consistent with ERSS predictions [7, 33].

The new arrangement of ideas presented here, i.e. areal/diametral measures, intrinsic/extrinsic factors, and the technique of using indentation shapes to give clues to extrinsic effects, therefore appears to be a fruitful approach for the future study of indentation-response anisotropy.

Acknowledgements

The authors wish to thank Professor Honeycombe for the provision of laboratory facilities, and the Science and Engineering Research Council for financial support for one of us (P.M.S.) during the period when this research was begun. Philip Burnett is thanked for providing the micrograph in Fig. 3. It is a pleasure to acknowledge Dr E. Yoffe's constructive critique of our manuscript.

References

1. "The Science of Hardness Testing and its Research Applications" (American Society for Metals, Ohio, 1973).
2. D. TABOR, "The Hardness of Metals" (Oxford University Press, Oxford 1951).
3. D. TABOR, *Rev. Phys. Technol.* **1** (1970) 145.
4. C. A. BROOKES, J. B. O'NEILL and B. A. W. REDFERN, *Proc. R. Soc. (London)* **A322** (1971) 73.
5. B. C. WONSIEWICZ and G. Y. CHIN, in "The Science of Hardness Testing and its Research Applications" (American Society for Metals, Ohio, 1973) p. 167
6. R. W. ARMSTRONG and A. C. RAGHURAM, in "The Science of Hardness Testing and its Research Applications" (American Society for Metals, Ohio, 1973) p. 174.
7. P. M. SARGENT, PhD thesis, University of Cambridge (1979).
8. D. M. MARSH, *Proc. R. Soc. (London)* **A279** (1964) 420.
9. C. A. BROOKES, R. P. BURNAND and J. E. MORGAN, *J. Mater. Sci.* **10** (1975) 2177.
10. A. G. ATKINS, in "The Science of Hardness Testing and its Research Applications" (American Society for Metals, Ohio, 1973) p. 223.
11. P. M. SARGENT and T. F. PAGE, *Scr. Metall.* **15** (1981) 245.
12. P. M. SARGENT and P. DONOVAN, *ibid.* **16** (1982) 1207.
13. N. H. MACMILLAN, in "Surface Effects in Crystal Plasticity", edited by R. M. Latanison and J. J. Fourie, NATO Advanced Study Institute Series E (Applied Science) No. 17 (1977) p. 629.
14. W. W. WALKER, in "The Science of Hardness Testing and its Research Applications" (American Society for Metals, Ohio, 1973) p. 258.
15. D. NEWEY, M. A. WILKINS and H. M. POLLOCK, *J. Phys. E* **15** (1982) 119.
16. A. R. C. WESTWOOD, J. S. AHEARN and J. J. MILLS, *Colloids Surf.* **2** (1981) 1.
17. C. J. STUDMAN, M. A. MOORE and S. E. JONES, *J. Phys. D* **10** (1977) 949.
18. E. YOFFE, *Phil. Mag.* **46A** (1982) 617.
19. M. G. S. NAYLOR and T. F. PAGE, *J. Microsc.* **130** (1983) 345.
20. B. R. LAWN and R. WILSHAW, *J. Mater. Sci.* **10** (1975) 1064.
21. T. F. PAGE, G. R. SAWYER, O. O. ADEWOYE and J. J. WERT, *Proc. Br. Ceram. Soc.* **26** (1978) 193.
22. B. R. LAWN, A. G. EVANS and D. B. MARSHALL, *J. Amer. Ceram. Soc.* **63** (1980) 574.
23. G. R. SAWYER, P. M. SARGENT and T. F. PAGE, *J. Mater. Sci.* **15** (1980) 1001.
24. C. A. BROOKES and R. P. BURNAND, in "The Science of Hardness Testing and its Research Applications" (American Society for Metals, Ohio, 1973) p. 257.
25. H. BUCKLE, in "The Science of Hardness Testing and its Research Applications" (American Society for Metals, Ohio, 1973) p. 453.
26. R. W. ARMSTRONG and C. Cm. WU, *J. Amer. Ceram. Soc.* **61** (1978) 102.
27. P. J. BLAU, *Scr. Metall.* **13** (1979) 95.
28. *Idem, ibid.* **14** (1980) 719.
29. M. A. VELEDNITSKAYA, V. N. ROZHANSKII, L. F. COMOLOVA, G. V. SAPARIN, J. SCHREIBER and O. BRUMMER, *Phys. Status Solidi* **A32** (1975) 123.
30. R. D. ARNELL, *J. Phys. D* **7** (1974) 1225.
31. Y. S. BOYARSKAYA, D. Z. GRABKO and E. I. PURICH, *J. Mater. Sci.* **14** (1979) 939.
32. G. W. GROVES and A. KELLY, *Phil. Mag.* **8** (1963) 877.
33. D. G. RICKERBY, *J. Amer. Ceram. Soc.* **62** (1979) 222.
34. D. LEE, in "The Science of Hardness Testing and its Research Applications" (American Society for Metals, Ohio, 1973) p. 147.
35. D. B. MARSHALL, T. NOMA and A. G. EVANS, *Comm. Amer. Ceram. Soc. C-176* **65** (1982).
36. I. C. LEIGH and G. N. PEGGS, National Physical Laboratory Report MOM 47 (NPL, Teddington, UK, 1980).
37. C. T. YOUNG and S. K. RHEE, *ASTM J. Test. Eval.* **6** (1978) 221.
38. Specimen from the work of D. C. Tidy and G. A. Chadwick, Dept. of Metallurgy and Materials Science, University of Cambridge (1967); see D. C. Tidy, PhD thesis, University of Cambridge (1970).
39. P. M. SARGENT and T. F. PAGE, *Proc. Br. Ceram. Soc.* **26** (1978) 209.
40. M. A. MOORE, PhD thesis, University of Newcastle upon Tyne (1974)
41. A. C. RAGHURAM and R. W. ARMSTRONG, *J. Less Common Met.* **22** (1970) 239.
42. F. W. CROSSMAN, A. S. YUE and A. E. VIDOZ, *Trans. AIME* **245** (1969) 397.
43. F. GIBERTEAU, A. DOMINGUEZ-RODRIGUEZ, R. MARQUEZ and J. CASTAING, *Rev. Phys. Appl.* **17** (1982) 777.
44. S. G. ROBERTS and T. F. PAGE, *J. Microsc.* **124** (1981) 77.

Received 16 April
and accepted 26 July 1984